Present Status and Physics Prospects of SSC

Shojiro SUGIMOTO

Osaka University
Toyonaka, Osaka 560, JAPAN.

September 30, 1989

ABSTRACT

Physics prospects of SSC are discussed, referring to other coming colliders. In addition, the present status of the SSC project and detector proposals for the experiments are described.

Talk given at the
meeting on 'Physics at TeV scale'
KEK, September 29-30 1989

1. SSC project

In order to study TeV region physics, several new colliders have been proposed: high energy p-p colliders with high luminosity, such as LHC and SSC, and high energy e^+e^- linear colliders, such as JLC. Among those proposals, Superconducting Super Collider (SSC) project has been approved and started first and foremost. The SSC collider with a circumference of eighty-seven kilometers is being designed to be constructed around Waxahachie, which town is situated about forty kilometers south of Dallas in Texas (fig.1). Head-on collisions of proton beams whirling around the tunnel in opposite directions are supposed to produce 1.7 interactions every 16 ns in the case of the maximum luminosity of $10^{33}cm^{-2}s^{-1}$ at $\sqrt{s}$=$40TeV$. Fig.2 shows a schematic for the SSC complex consisting of five accelerators: LINAC, LEB (low energy booster), MEB (medium energy booster), HEB (high energy booster), and the $20TeV$–$20TeV$ SSC collider. A schedule for the SSC construction is shown in fig.3, where the first beam collisions are expected at the beginning of 1999. The SSC parameters[1] are summarized in table 1.

2. Comparison between SSC and other coming colliders

Physics interests at the SSC are listed in table 2,[2] where the expected event rates and their observabilities are also shown. Another future p-p collider, LHC[3] of CERN, is expected to be approved in a few years and to come into operation in 1997. The designed luminosity of the LHC, although the maximum energy is low, is much higher than that of the SSC as shown in table 1.

On the other hand, electron-positron linear colliders such as JLC could efficiently produce clean events in the TeV region. Comparing[4] effective center-of-mass energies of e^+e^- and p-p collisions, one can clearly see a merit of those hadron colliders (fig.4). Figure 5, summarized by U.Amaldi,[5] shows the discovery limits for 12 different processes at hadron and e^+e^- colliders. One of the most important studies to confirm the standard model is certainly the Higgs particle search, but the discovery limit is not so high at the SSC in comparison with at the other colliders because of the mass width growing as M_h^3 and of the QCD backgrounds. From the point of view of the standard theory, the Higgs

mass should be below 1 TeV/c^2. If the mass does not exist in the region, the WW interactions are expected to be strong in TeV region and hence new physics will show up.

Among various physics interests in the TeV region, the discovery limits for heavy gauge bosons at the SSC are extremely high in comparison with the proposed electron-positron colliders, as shown in fig.5. Therefore the new gauge boson search at the SSC is one of the most interesting themes.

3. Gauge Boson Physics

(a) Why gauge boson ?

To confirm the standard model, we have to test gauge couplings in the vertices of WWZ, $WW\gamma$, and four vector-bosons (fig.6).[6] If the Higgs particle does not exist below 1 TeV, the perturbative WW scattering amplitude violates unitarity at $\sqrt{s} \geq 1.7 TeV$ and thus the interaction becomes strong. Fig.7 shows an invariant mass distribution for pp $\rightarrow W^+W^-X$ in the case of $M_h = 1 TeV$.[7] Recently M.Chanowitz has reviewed WW scattering at $M_{WW} > 1 TeV$, and has estimated the event rates and their backgrounds. In addition, he suggested attractive scattering processes of W^+W^+ and W^-W^- which have no $q\bar{q}$ annihilation background.[8] Therefore gauge boson detections at the SSC are essential to study the symmetry-breaking mechanism in the TeV region.

(d) Extra W

In the standard model based on $SU(2)_L$ x $U(1)$, $W^{\pm}$ couples to only doublets of left-handed quarks or leptons. If we extend the frame of the standard model to $SU(2)_L$ x $SU(2)_R$ x $U(1)_{L-B}$, new right-handed W_R will be required in the left-right symmetric model. An estimated P_T distribution of single electrons/pions decayed from 1000GeV $W^{\pm}$s is shown in fig.8.[9]

(e) W Polarization

If the new $W^{\pm}$ exists in the TeV region, the helicity has to be investigated by using charge asymmetry of pions from τ in the process of $W_{L/R} \rightarrow \tau\nu_\tau$ (fig.9).

(f) Extra Z

We do not know the reason why the number of generations is only three, and how the generations appear. If horizontal gauge bosons or superstring gauge bosons exist, the new particles are detectable with an electromagnetic calorimeter or a muon tracker (fig.10). [10]

(g) Determination of the Mixing Angle α

If new Z particles exist in the TeV region, the mixing angle can be measured by the method shown in fig.11.

4. Detectors

Muons as well as electrons are the most important signals at SSC experiments, because those are expected to uncover the existence of neutral Higgs, sequential heavy quarks, heavy leptons, leptoquarks, extra/ordinary Z, W, etc.

Solenoid 4π detectors[11] (fig.12), a non-magnetic detector[12] (EMPACT: fig.13), and a large magnetic detector[13,14] (L*: fig.14) have been proposed. Their expected momentum resolutions for electrons and muons are shown in the above table, where the resolutions of electrons are expected to be much better than those of muons. But the practical resolution of electrons may become worse because of the systematic error, electronics noise, event noise (minimum bias events), signal pile-up and/or pedestal variation, track overlap, etc. Those effects may be serious below a few hundred GeV/c for rare events which we are interested in.

For muons, two kinds of detection schemes, so far, are proposed for SSC experiments. The solenoid 4π detectors measure produced muon momenta inside the magnet, identify muons with the filter, and could measure their momenta outside the calorimeter if the iron filters are magnetized. On the other hand EMPACT and L* precisely measure muon momenta outside the calorimeters, correct the momenta using the information of energy deposit in the calorimeters, and determine the production angles with the inner trackers.

EMPACT intends to precisely measure muons as well as electrons and jets over the large solid angle with the air-core toroids, which generate a purely azimuthal field always perpendicular to the trajectories. The detector is shown in fig.13.

L*, based on the L3, consists of a large solenoid, calorimeters, and an excellent muon chamber system. The group is also investigating other choices, namely radially distributed toroidal coils (fig.14) and "magnetic bottle". A typical Higgs event and a minimum bias event in a solenoid detector are shown in fig.15.

5. Summary

It is extremely interesting to investigate the symmetry-breaking mechanism in TeV region, with the coming high energy colliders. To perform those studies, we have to carefully design the detectors most suitable to the processes.

References

1. H.Edwards, *Status Report SSC Design.* Talk presented at the International Conference on High Energy Accelerators, Tsukuba, August 20-26 1989
2. T.Kondo, *SSC.* Proc. Workshop on Hadron Collider Physics, Univ. of Tokyo, Jan. 12-13, 1987.
3. G.Brianti, *The Large Hadron Collider (LHC) in the LEP Tunnel.* Talk presented at the ECFA/CERN/CICYT/EEC workshop, Barcelona, September 14-21 1989, CERN-89-10 (vol.I) 13
4. C.Ahn et al., *Opportunities and Requirements for Experimentation at High Energy e^+e^-* Collider. SLAC-Report-329, May 1988
5. U.Amaldi et al., *Summary of the Discovery Limits Expected for 12 Different Processes.* Proc of the Workshop on Physics at Future Accelerators, La Thuile and Geneva, 1987, CERN-87-07 (vol.I) 323
6. D.Zeppenfeld, "Substructure and Horizontal Symmetries at Hadron Colliders," *Internal Journal of Modern Physics A*, vol. 2-4, pp. 1273-1284, World Scientific Publishing Company, 1987. Proc. Workshop 'From Collider to Super Colliders', Wisconsin, May 11-12 1987.
7. D.A.Dicus and R.Vega, "WW Production from pp Collisions," *Physical Review Letters*, vol. 57-9, pp. 1110-1112, The American Physical Society, 1 September 1986.
8. M.S.Chanowitz, "Electroweak Symmetry Breaking: Unitarity, Dynamics, and Experimental Prospects," *Ann. Rev. Nucl. Part. Sci.*, vol. 38, pp. 323-420, Annual Reviews Inc., 1988.
9. J.F.Gunion and H.E.Haber, τ-decay Spectra at the SSC. Snowmass 84, p150
10. V.Barger et al., *Signature for Extra Gauge Bosons of E_6* at the SSC. Snowmass 86, p224.
11. G.G.Hanson et al., *Large Solenoid Detector.* Proc. of the Workshop on Experiments, Detectors and Experimental Areas for the Supercollider, Berkely, 1987, 340.
12. M.Marx, *EMPACT.* SSC-219, May 1989
13. U.Becker et al., *L3+1.* Proc. of the Workshop on Experiments, Detectors and Experimental Areas for the Supercollider, Berkely, 1987, 525.
14. M.Chen and P.Marston, *Magnetic Bottles: to Improve Resolution of Solenoids at Hadron Colliders.* MIT-LNS Report No.172, June 1989

Collider parameter	SSC	LHC(low)	LHC(high)
E(TeV)	20(for $6.55T$)	8(for $10T$)	8(for $10T$)
Circumference	87,120m	26,659m	26,659m
N(10^{10} protons/bunch)	0.75	2.9	10
N(bunches/ring)	17,424	3,120	4,810
BN(10^{13} protons/ring)	13	9.1	48.1
$F_{ROTATION}$	3.4 kHz	11.246 kHz	11.246 kHz
$F_{COLLISIONS}$	60MHz	35MHz	54MHz
Transv. Emitt.($10^{-6} radmm$)	1	25	15
$S_{BUNCH-SEPARATION}$	5.0 m	8.5 m	5.5 m
$T_{BUNCH-SEPARATION}$	16 ns	29 ns	18 ns
Bunch Length	6-7.3cm(σ)	31cm(4σ)	31cm(4σ)
β^*(m)	0.5	0.25	0.25
Luminosity ($10^{33} cm^{-2} s^{-1}$)	1-(5)	6.2	37.9
Luminosity/hit ($10^{25} cm^{-2} s^{-1}$)	1.6		

Table 1. P-P Collider Parameters

Ref.1. Ref.3.

class	process	physics	observability	event rate $L=10^{33}cm^{-2}s^{-1}$, $10^7 s/year$
QCD	$PP\rightarrow jets$	*QCD test* *compositeness* *luminosity monitor*	*high* P_T *jet* *detectable with* *calorimeters*	1 *event/sec* *at* P_T=2 *TeV*
standard *Electro–* *Weak* *Theory*	$PP\rightarrow l^+l^-$	*QCD study* *heavy quark search*	e^+e^-, $\mu^+\mu^-$ $\tau^+\tau^-$?	10 *events/year* *at* m_{ll}>3 *TeV*
	$W^{\pm}X$	*prod. mechanism* P_T *depencences*	$W\rightarrow l\nu$ (16%×2) $W\rightarrow$ *hadrons* ?	2×10^9 $W^{\pm}$ */year*
	Z^0X	*rare decay modes* *QCD test*	$Z\rightarrow l^+l^-$ (3%×2) $Z\rightarrow$ *hadrons* ?	6×10^8 Z^0 */year*
	$W^{\pm}W^{\pm}$	*trilinear coupling*	$WW\rightarrow(h)(l\nu)$?	10^6 WW*/year*
	$W^{\pm}Z^0$	*non–standard intr.*	$WZ\rightarrow(l\nu(32\%))(l^+l^-(6\%))$	$5\times10^5 WZ$*/year*
	Z^0Z^0	*bkgd for Higgs search*	$ZZ\rightarrow(l^+l^-(6\%))(l^+l^-(6\%))$	$2\times10^5 ZZ$*/year* $\rightarrow$700 $l^+l^-l'^+l'^-$
	$W^{\pm}\gamma$	*mag. moment of* W	$W^{\pm}\gamma\rightarrow(l\nu)$(*isolated* γ)	$10^4 W^{\pm}\gamma(>200GeV)$*/year*
	$Z^0\gamma$	*anomalous intr.*	$Z^0\gamma\rightarrow(l^+l^-)$(*isolated* γ)	$10^5 Z^0\gamma(>200GeV)$*/year*
	prompt γ	*QCD test(high* P_T^{γ}*)* $G(X,Q^2)$ *determ.*	γ/π^0>1 for $X_T\geq$.02–.03 *isolated* γ	$10^5\gamma$*/year* *for* P_T^{γ}>0.5 *TeV*
	H^0	*Higgs search* .2 *TeV*/c^2–1 *TeV*/c^2	$H\rightarrow W^{\pm}W^{\pm}\rightarrow(e\nu)(jet)$ S/N=0.1–0.3	400 */year* *jet* + $l\nu$ *at* M_H=400 *GeV*
			$H\rightarrow Z^0Z^0\rightarrow llll$ $S/N\geq$4	10 */year* $llll'l'$ *at* M_H=400 *GeV*
	$H^0W^{\pm}$ H^0Z^0	*Higgs search with* *less bkgd*	$HW\rightarrow(WW)W$ *six jets detect.* ?	$10^3 HV$ *pairs/year* *at* M_H=400 *GeV*

class	process	physics	observability	event rate $L=10^{33}cm^{-2}s^{-1}$, $10^7 s/year$
New	$Q\overline{Q}$	*heavy quark search*	$Q\overline{Q}\rightarrow(qW)(jets)$ $\rightarrow(jets\ l\nu)(jets)$, *high* p_t l	100 */year* *at* M_Q=2.5 *TeV*
	$L^{\pm}L^{\pm}$	*heavy lepton search*	$L^+L^-\rightarrow(W^+N^0)(W^-N^0)$ P_T *imbalance*	100 */year* *at* M_Q=600 *GeV*
	$L^{\pm}N^0$	*heavy lepton search*	$L^{\pm}N^0\rightarrow(W^{\pm}N^0)N^0$ P_T *imbalance*	×10 *of* $L^{\pm}L^{\pm}$
	W'	*new Electro−Weak bosons*	$W'\rightarrow e\nu_e$, $\mu\nu_\mu$ *or* $\rightarrow$*jet jet* ?	10^4 */year* *at* 4 *TeV*
	Z'		$Z^{0\prime}\rightarrow e^+e^-$, $\mu^+\mu^-$ *or* $\rightarrow$*jet jet* ?	10^4 */year* *at* 4 *TeV*
SUSY	$\tilde{g}\tilde{g}$ $\tilde{q}\tilde{g}$ $\tilde{q}\tilde{q}$	*SUSY search*	*missing* P_T *hard photon*	2000 $\tilde{g}\tilde{g}$ */year* *at* $M_{\tilde{g}}$=2 *TeV*
	$\tilde{g}\tilde{\gamma}$ $\tilde{g}Z^0$ $\tilde{g}W^{\pm}$	*SUSY search*	*missing* P_T *hard photon*	100$\tilde{g}\tilde{\gamma}$/*year* *at* $M_{\tilde{g}}$=1 *TeV*
Techni−color	ρ_T^0 $\rho_T^{\pm}$ ..	*technicolor search*	$\rho_T^{0,\pm}\rightarrow W^+W^-$, WZ *enhancement in jet pair mass* ?	240 */year* *at* M_{ρ_T}=1.8 *TeV*
composite	q^*	*excited quark search*	$q^*\rightarrow\gamma q$, *inv. mass meas.*	10^4 */year* *at* M_{q^*}=1 *TeV*

Table 2. Hard Scattering at $\sqrt{s}$= 40TeV

Ref.2.

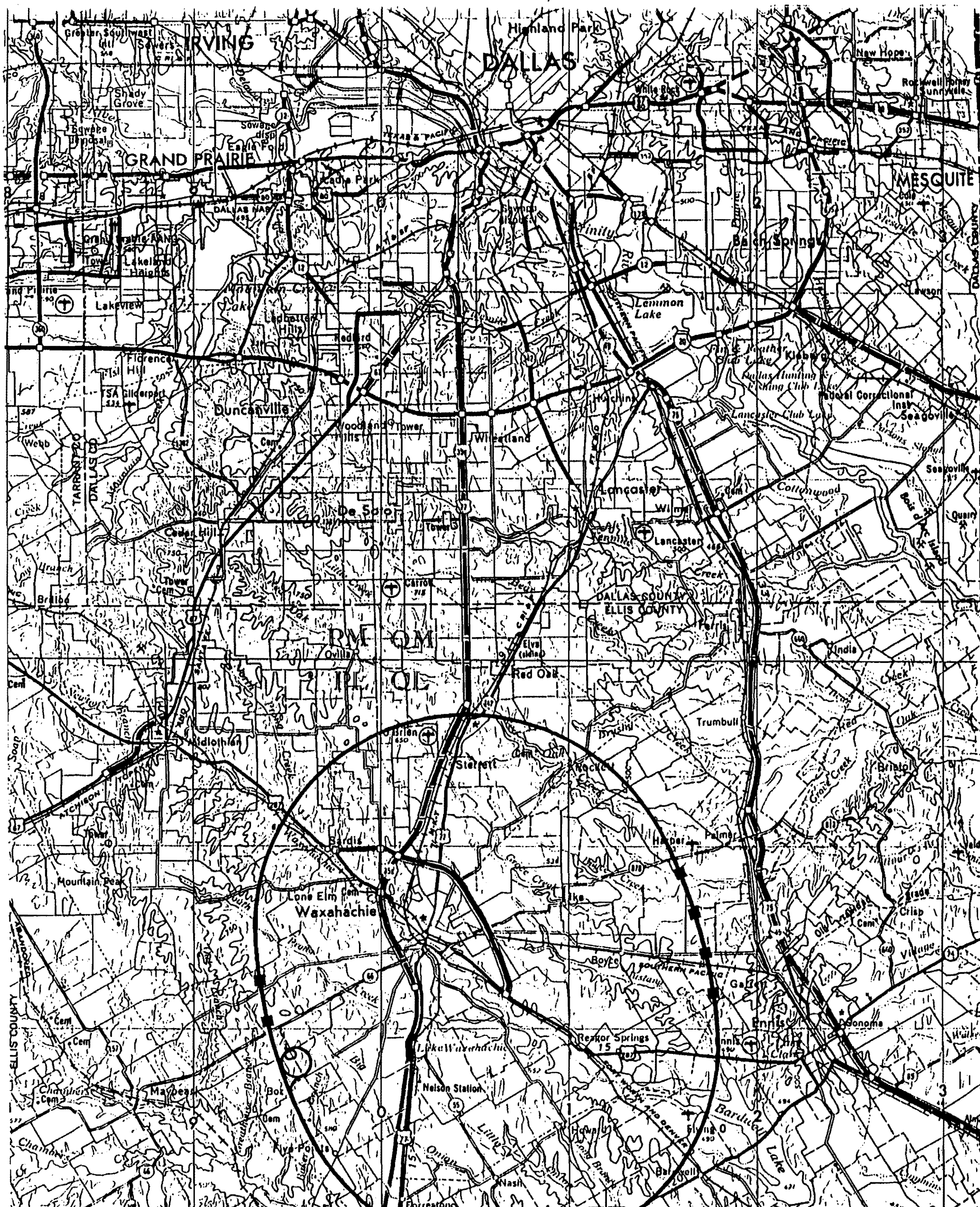

Fig.1.

SSC - SCHEMATIC

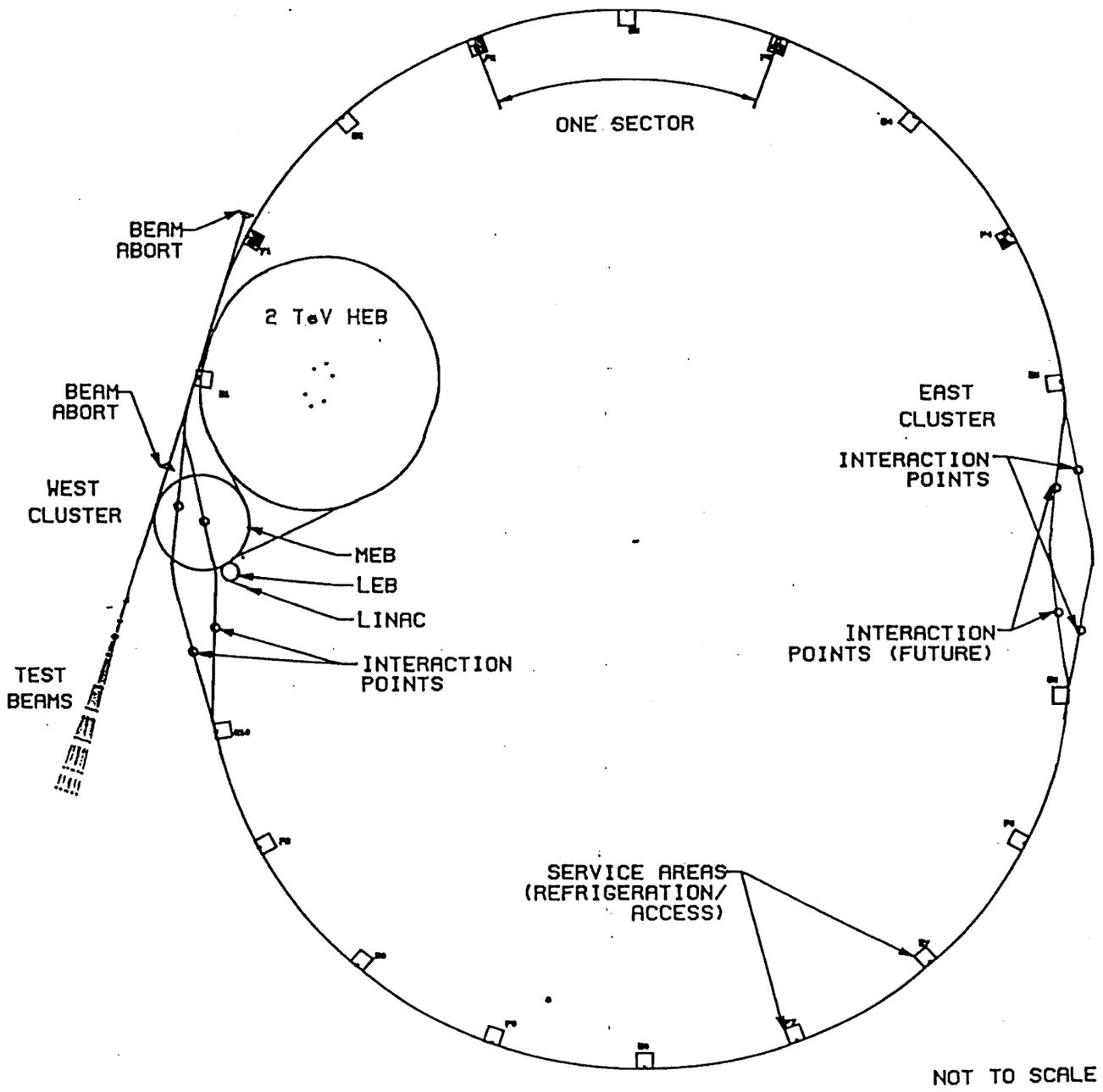

Fig.2.

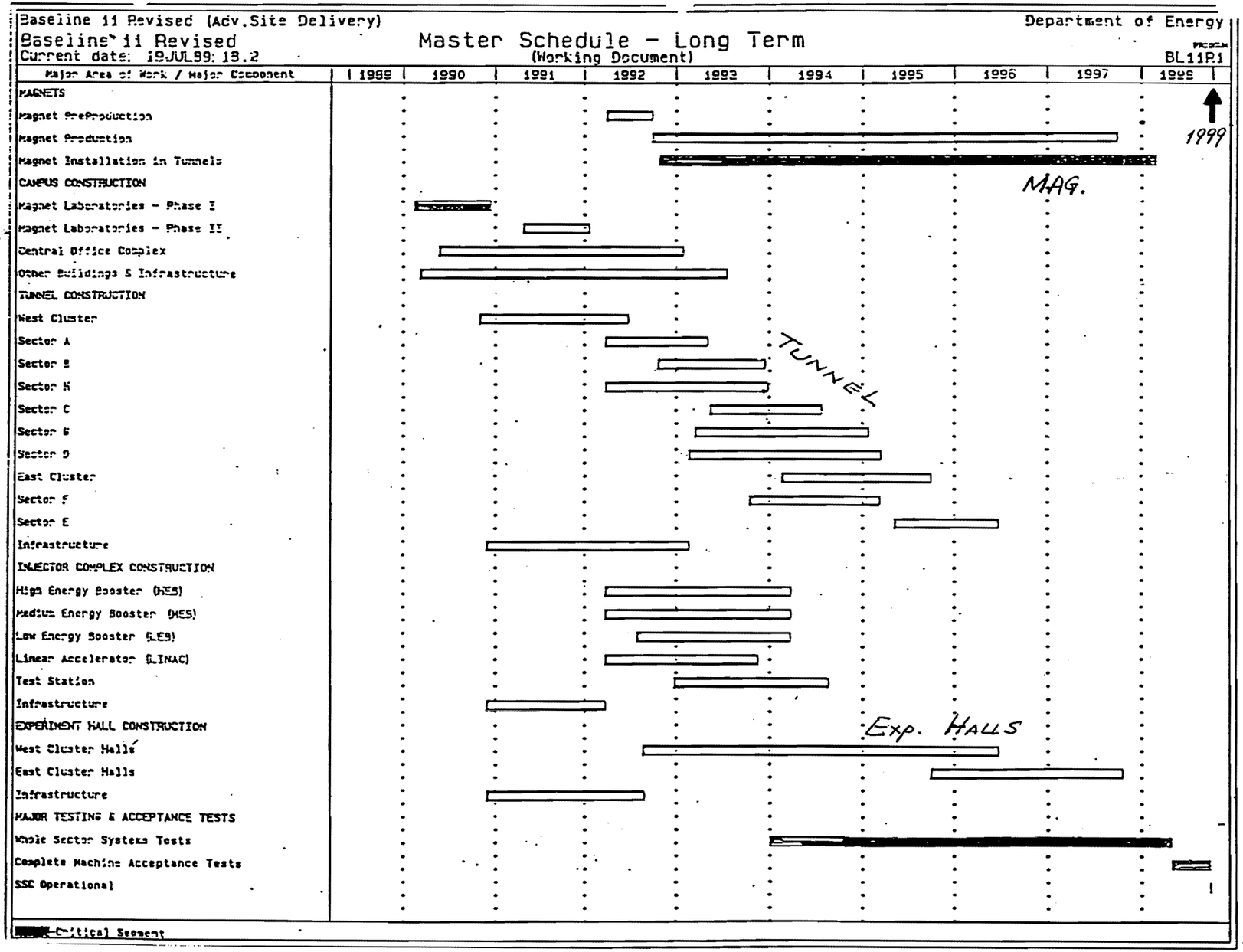
Baseline 11 Revised (Adv.Site Delivery)
Baseline 11 Revised
Current date: 19JUL89: 13.2
Master Schedule - Long Term
(Working Document)
Department of Energy
BL11R1
Major Area of Work / Major Component
1988
1990
1991
1992
1993
1994
1995
1996
1997
1998
1999
MAGNETS
Magnet PreProduction
Magnet Production
Magnet Installation in Tunnels
CAMPUS CONSTRUCTION
Magnet Laboratories - Phase I
Magnet Laboratories - Phase II
Central Office Complex
Other Buildings & Infrastructure
TUNNEL CONSTRUCTION
West Cluster
Sector A
Sector B
Sector H
Sector C
Sector G
Sector D
East Cluster
Sector F
Sector E
Infrastructure
INJECTOR COMPLEX CONSTRUCTION
High Energy Booster (HEB)
Medium Energy Booster (MEB)
Low Energy Booster (LEB)
Linear Accelerator (LINAC)
Test Station
Infrastructure
EXPERIMENT HALL CONSTRUCTION
West Cluster Halls
East Cluster Halls
Infrastructure
MAJOR TESTING & ACCEPTANCE TESTS
Whole Sector Systems Tests
Complete Machine Acceptance Tests
SSC Operational
MAG.
TUNNEL
Exp. HALLS
Critical Segment

Fig.3.

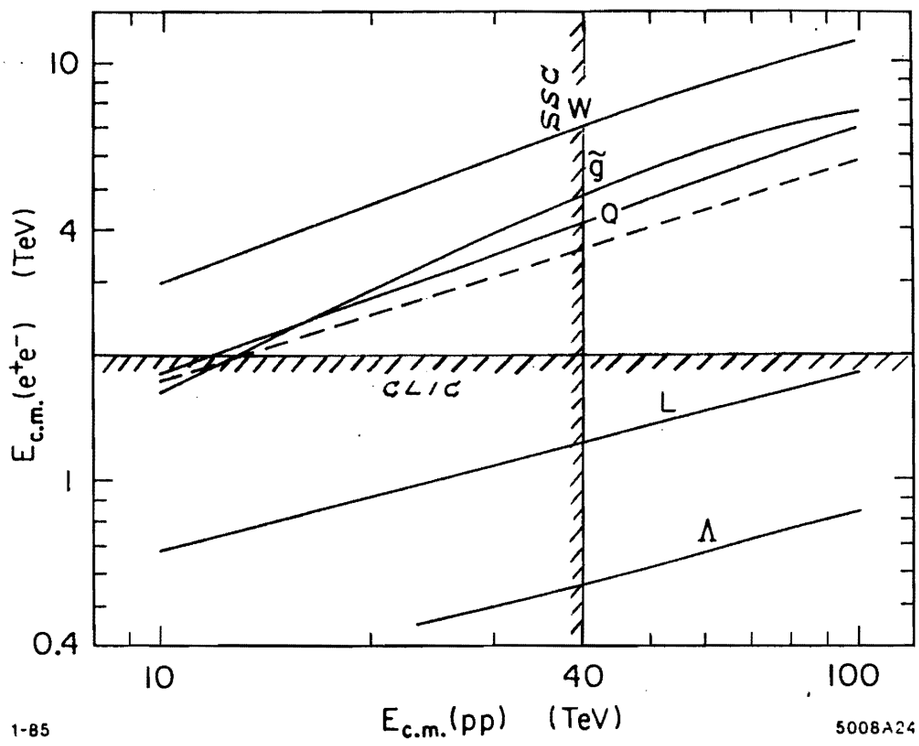

Fig.4. Comparison of effective center of mass energies of e^+e^- and pp colliders for discovering various hypothesized new particles, assuming a maximum pp luminosity of 10^{33} $cm^{-2}sec^{-1}$. The searches considered are those for new vector bosons, supersymmetry partners, heavy quarks, heavy leptons, and fermion compositeness. The dashed line represents eq. $E_{CM}(e^+e^-) = \sqrt{E_{CM}(PP)/3}$.

Ref.4.

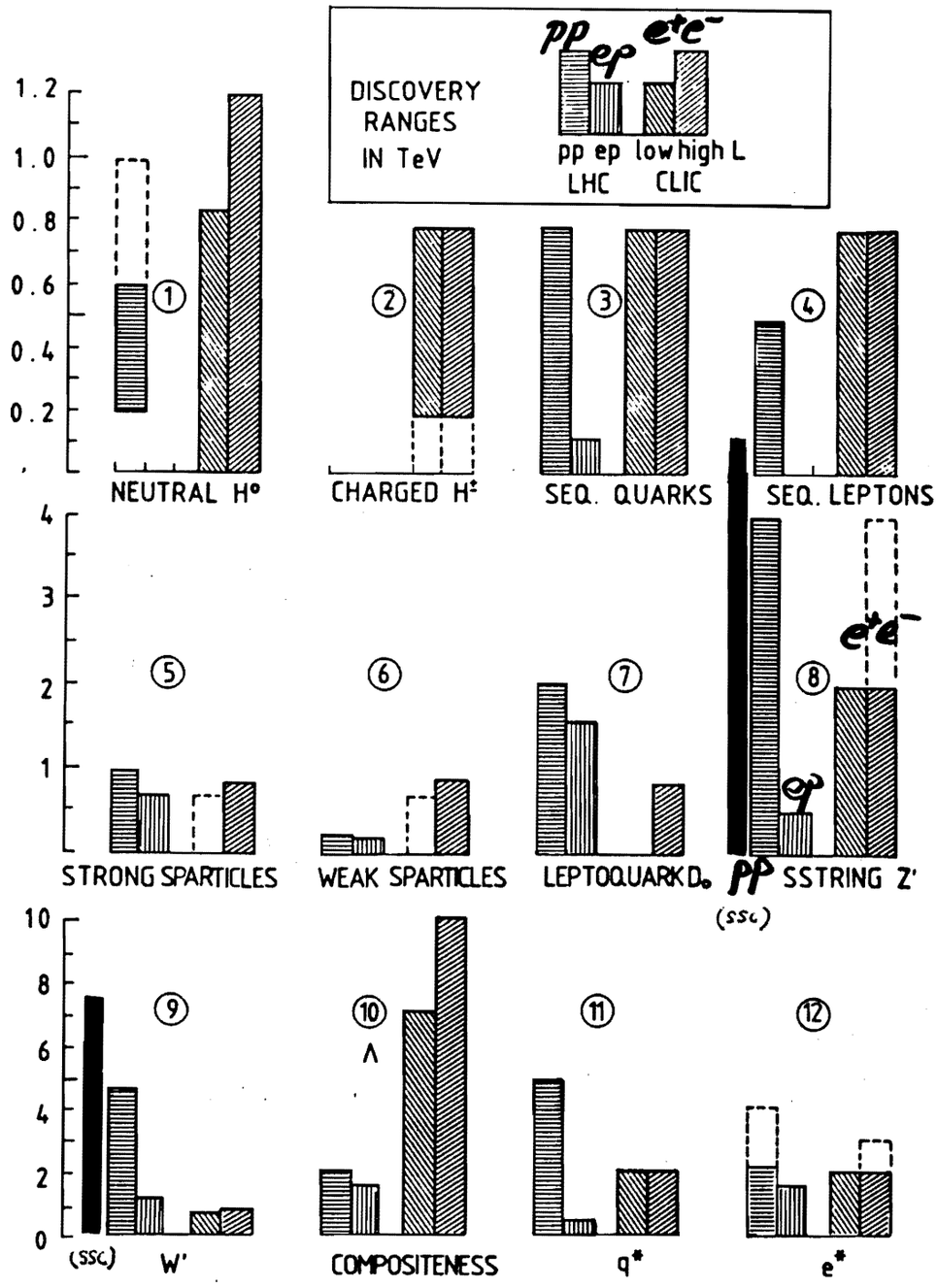

Fig.5. Summary of the discovery limits expected for 12 different processes. The vertical scale is in TeV and changes by a factor of 4 (2.5) when passing from the first (second) to the second (third) line. The four dashed areas in each diagram refer to the following beam conditions, from left:
proton-proton at $E_{cm} \simeq 16$ TeV with $L \simeq 10^{33}\,cm^{-2}\,s^{-1}$;
electron-proton at 1.5 TeV with $L \simeq 10^{32}\,cm^{-2}\,s^{-1}$;
electron-positron at 2 TeV with $L \simeq 10^{33}\,cm^{-2}\,s^{-1}$ (indicated for simplicity as 'low' L);
electron-positron at 2 TeV with $L \simeq 4 \times 10^{33}\,cm^{-2}\,s^{-1}$ ('high' L).
The detailed explanations of the 12 histograms are given in the text. Note that in working out the discovery limits and in compiling the figures all the quoted luminosities have been taken for granted, even if the CLIC electron-positron collider is still at the level of a 'conceptual design'.

Ref.5.

EXPECTED SPECTRA

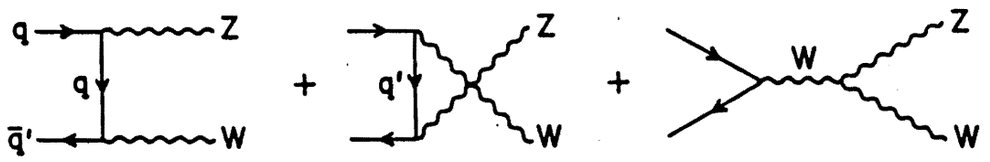

Fig. 7: Feynman graphs for ZW production.

$$\mathcal{L}_{eff} = g_{WWZ}\Big\{ig_1(W^\dagger_{\mu\nu}W^\mu Z^\nu - W^\dagger_\mu Z_\nu W^{\mu\nu}) + i\kappa W^\dagger_\mu W_\nu Z^{\mu\nu} + \frac{i\lambda}{m_W^2}W^\dagger_{\lambda\mu}W^\mu{}_\nu Z^{\nu\lambda} + g_5\epsilon^{\mu\nu\rho\sigma}(W^\dagger_\mu \overleftrightarrow{\partial}_\rho W_\nu)Z_\sigma - g_4 W^\dagger_\mu W_\nu(\partial^\mu Z^\nu + \partial^\nu Z^\mu) + i\tilde{\kappa}W^\dagger_\mu W_\nu \tilde{Z}^{\mu\nu} + \frac{i\tilde{\lambda}}{m_W^2}W^\dagger_{\lambda\mu}W^\mu{}_\nu \tilde{Z}^{\nu\lambda}\Big\}. \quad (9)$$

Here W_μ is the W^- field, $Z^{\mu\nu} = \partial^\mu Z^\nu - \partial^\nu Z^\mu$ and $\tilde{Z}^{\mu\nu} = \frac{1}{2}\epsilon^{\mu\nu\rho\sigma}Z_{\rho\sigma}$. Among these couplings g_4, $\tilde{\kappa}$ and $\tilde{\lambda}$ are CP violating while g_5 violates C and P but is CP even.

Choosing the overall coupling constant as $g_{WWZ} = -e\cot\theta_W$, the S.M. predicts all the couplings in (9) to vanish at tree level except for $g_1 = 1$ and $\kappa = 1$.

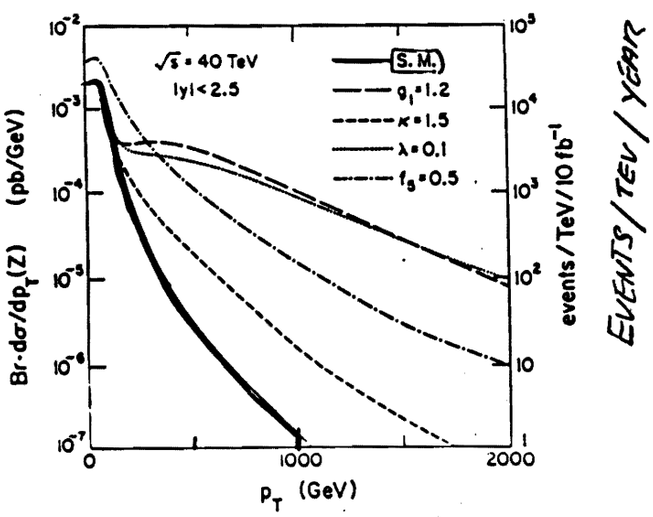

p_T distribution of the Z's produced in $pp \to ZW^+ + X$ at $\sqrt{s} = 40$ TeV. for various deviations from the S.M. ZWW vertex. The branching ratio for both the W and the Z decaying into electrons or muons is included. All charged leptons satisfy $|y| < 2.5$. The scale on the right gives the number of events per TeV expected after one year of running with a luminosity of $10^{33}\text{cm}^{-2}\text{sec}^{-1}$.

Fig.6 Ref.6.

$qq \rightarrow \begin{cases} W^+W^- \\ qqW^+W^- \end{cases}$

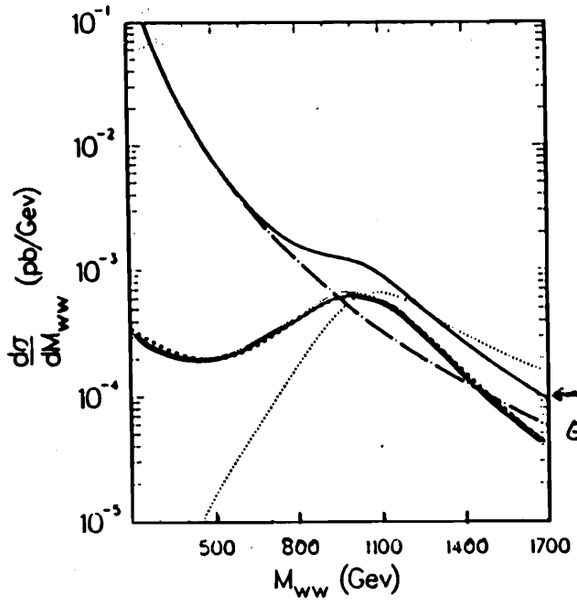

1 ssc year
↓
$10^4 pb^{-1}$

$WW \rightarrow (l\nu)(jet\,jet)$
ε 0.94 ~92-0.4
BR 0.16 0.75
← 2-4 Detection Eff. ~0.02-0.04
Events/100GeV

The invariant-mass distribution for $pp \rightarrow W^+W^-X$. M_{WW} is the invariant mass of the two W's. $\sqrt{s}$ is 40 TeV, the rapidity cut is fixed at 1.5, and the Higgs-boson mass is taken to be 1 TeV. The dot-dashed line is the background from $qq \rightarrow W^+W^-$. The dashed line is the contribution from $qq \rightarrow qqW^+W^-$. The solid line is the total of these two contributions. The dotted line is the contribution from the s-channel Higgs-boson pole in $qq \rightarrow qqW^+W^-$ only.

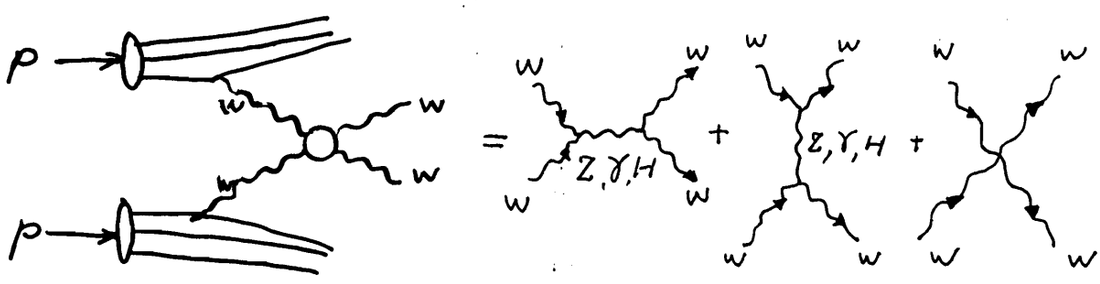

Fig.7. Ref.7.

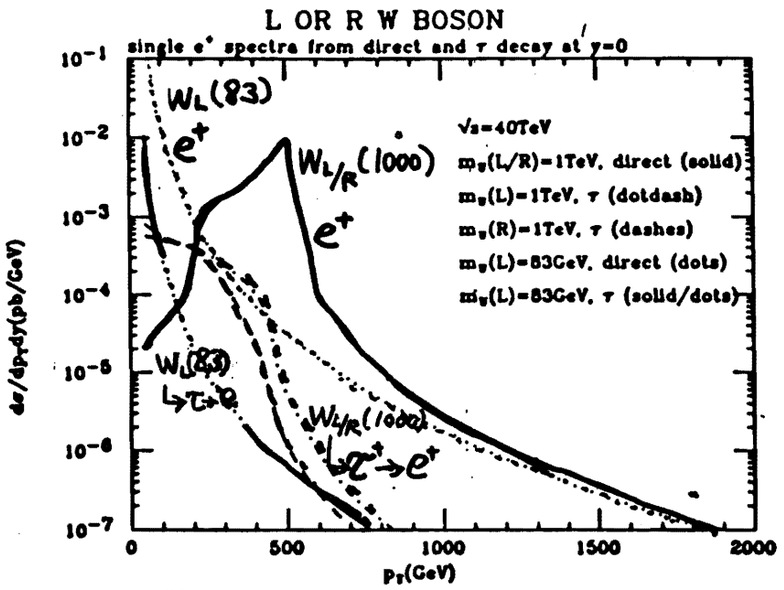

Single e^+ spectra from $W^+(83)$ and new W_L^+, W_R^+.

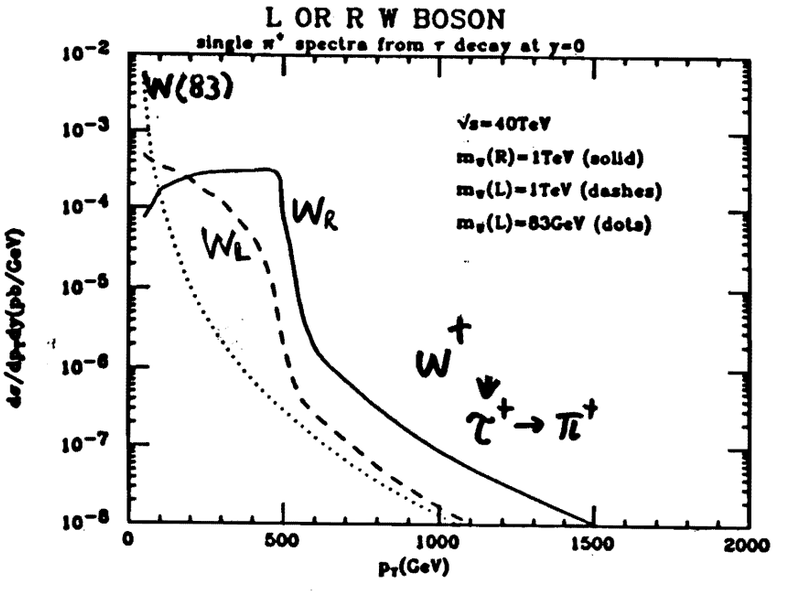

Single π^+ spectra from $W^+(83)$ and new W_L^+, W_R^+.

Fig.8. Ref.9.

V. DETERMINATION OF THE W_E POLARIZATION

W_E POLARIZATION
↓
τ POLARIZATION
↓
τ DECAY ANGULAR DISTRIBUTION

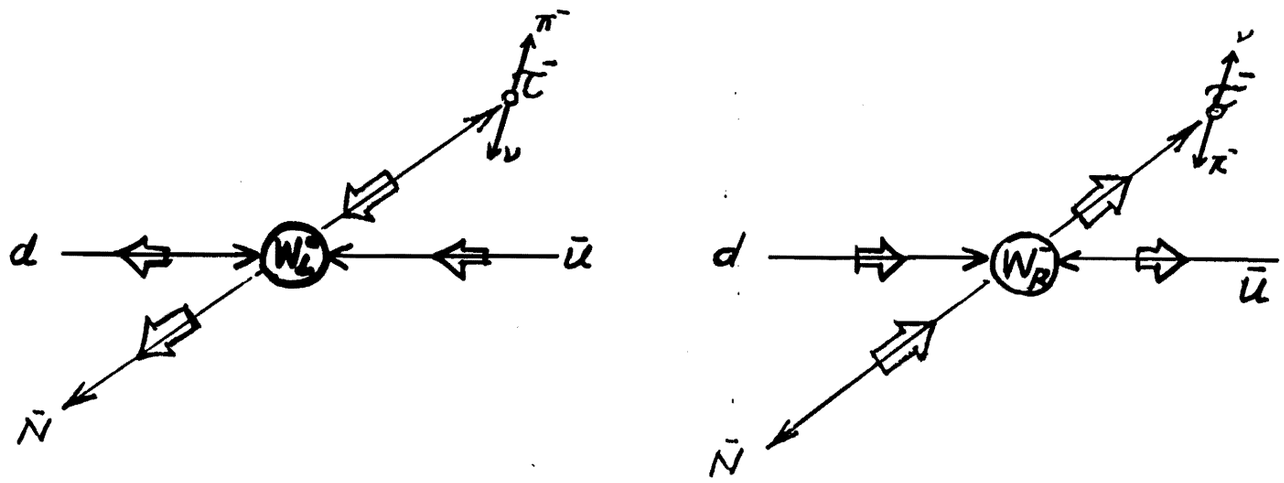

(a) High P_T electron detection

$(pp \to W'X \to \tau X' \to eX'')$ IS NOT DETECTABLE

BECAUSE OF THE BACKGROUND FROM $(pp \to W/W' X \to eX')$.

(b) High P_T PION detection

$(pp \to W'X \to \tau X' \to \pi X'')$ IS PROMISING.

Fig.9.

VI. Extra Z (Z_E) Search

Z_E Decay	B.R.* (Z_η)	Event Shape (r-φ view)
$\to q\bar{q}$	72.4% (~80%)	Z_E: $\bar{q}$ — q
$\to l^+l^-$	9.2% (~13%)	Z_E: l^+ — l^-
$\to \nu\bar{\nu}$	18.4% (~7%)	Z_E: ν — $\bar{\nu}$

* Assuming the same coupling as Z (936 GeV)

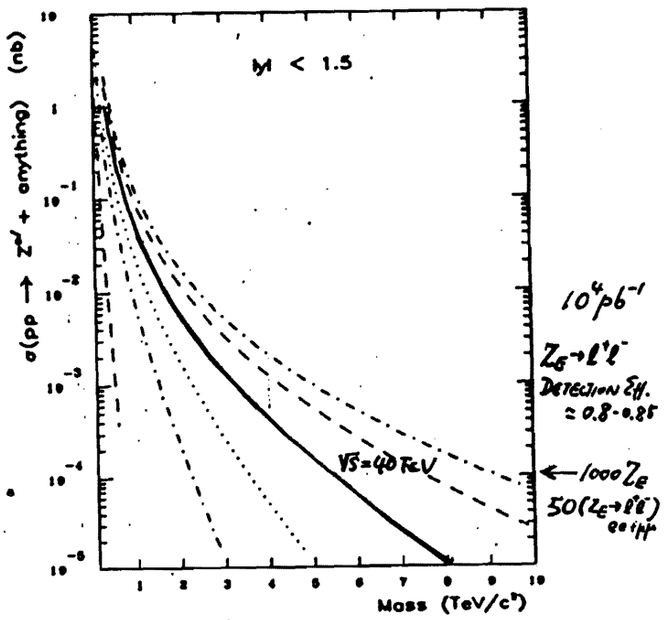

Integrated cross sections for the production of Z^α with rapidity $|y_{Z^\alpha}| < 1.5$ in proton-proton collisions, according to the parton distributions of Set 2.

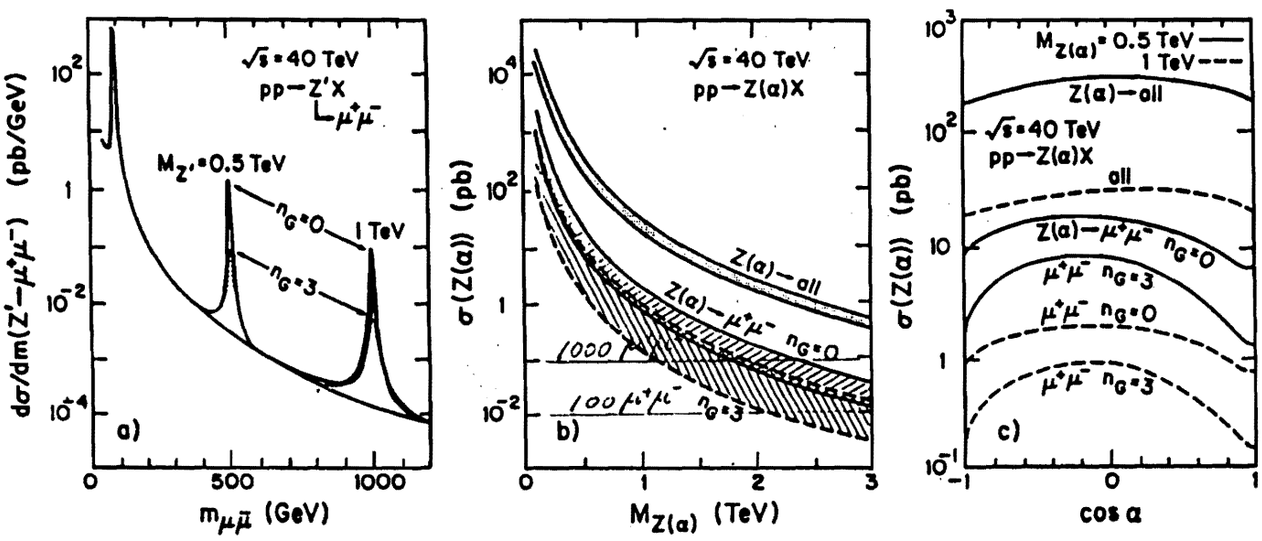

Fig.10. Predictions for Z' ($\cos\alpha = \sqrt{5/8}$) production in a pp collider at $\sqrt{s} = 40$ TeV: (a) $d\sigma/dm(pp \to e^+e^-X)$ versus dilepton invariant mass for $M_{Z'} = 0.5$ and 1 TeV; the solid (dotted) curves correspond to $n_G = 0$ (3); (b) σ and $\sigma B(Z(\alpha) \to e^+e^-)$ for producing $Z(\alpha)$ versus $M_{Z(\alpha)}$; the shaded regions correspond to the range allowed by α; (c) σ and $\sigma B(Z(\alpha) \to e^+e^-)$ for $M_{Z(\alpha)} = 0.5$ and 1 TeV versus $\cos\alpha$.

Ref.10.

VII. Determination of the Mixing Angle α

— By Measuring F-B Asymmetry in $Z_E \to \ell^+\ell^-$ —

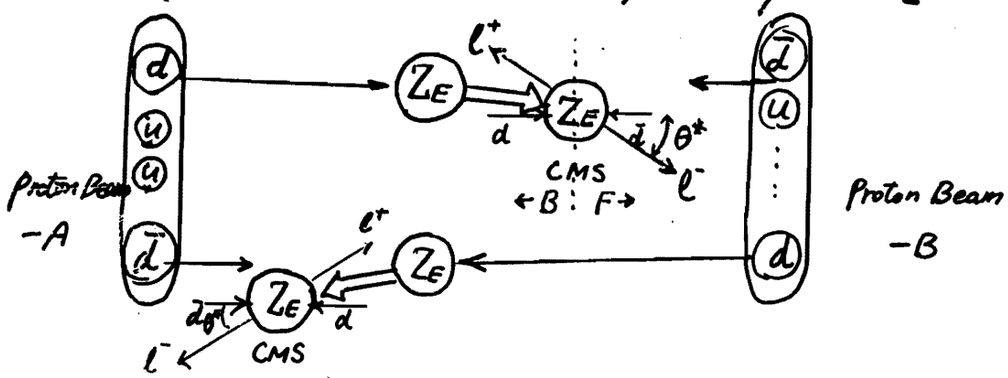

Differential cross section $f\bar{f} \to e^+e^-$ can be written as

$$\frac{d\sigma^{f\bar{f}}}{d\cos\theta^*} = (S_f(1+\cos^2\theta^*) + 2A_f\cos\theta^*)$$

near the $Z_{(\alpha)}$ resonance, $S_f, A_f = \frac{m^4}{(m^2-M^2_{Z(\alpha)})^2+M^2_{Z(\alpha)}\Gamma^2_{Z(\alpha)}} \cdot \frac{(g_L^2(e)\pm g_R^2(e))(g_L^2(f)\pm g_R^2(f))}{4\cos^2\theta_W}$

Hadronic cross section for $A+B \to e^+e^-X$ is written as

$$\frac{d\sigma}{dm\,dy\,d\cos\theta^*} = \frac{\pi\alpha_{em}^2 x_A x_B K}{3m^3}\sum_q (S_q(1+\cos^2\theta^*)G_q^+ + 2A_q\cos\theta^* G_q^-)$$

$$G_q^\pm(y, m^2, s) = f_{q/A}(x_A) f_{\bar{q}/B}(x_B) \pm f_{\bar{q}/A}(x_A) f_{q/B}(x_B)$$

$$A^{FB}(y) = \frac{d\sigma^F/dy - d\sigma^B/dy}{d\sigma^F/dy + d\sigma^B/dy} = \frac{3}{4}\frac{g_L^2(e)-g_R^2(e)}{g_L^2(e)+g_R^2(e)}\cdot\frac{(g_L^2(q)-g_R^2(q))G_q^-}{(g_L^2(q)+g_R^2(q))G_q^+}$$

→ extra U(1) charge → f(α)

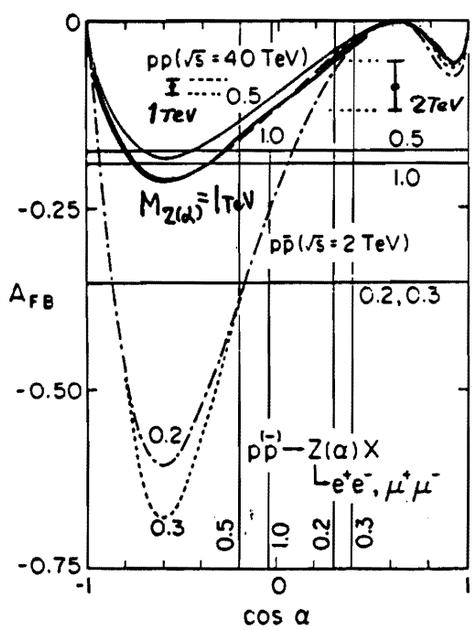

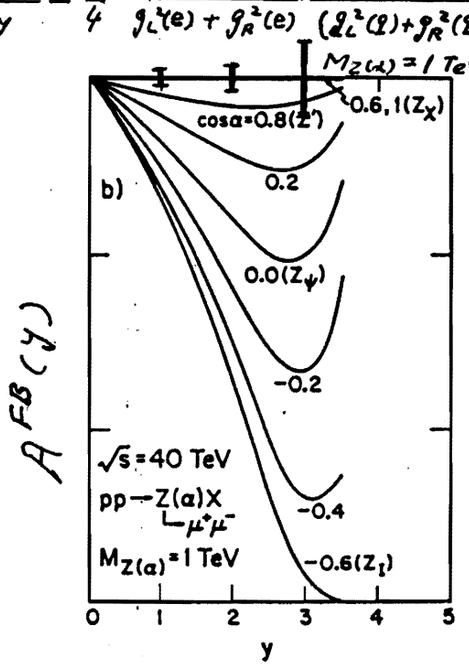

ISAJET Simulation

Fig.11.

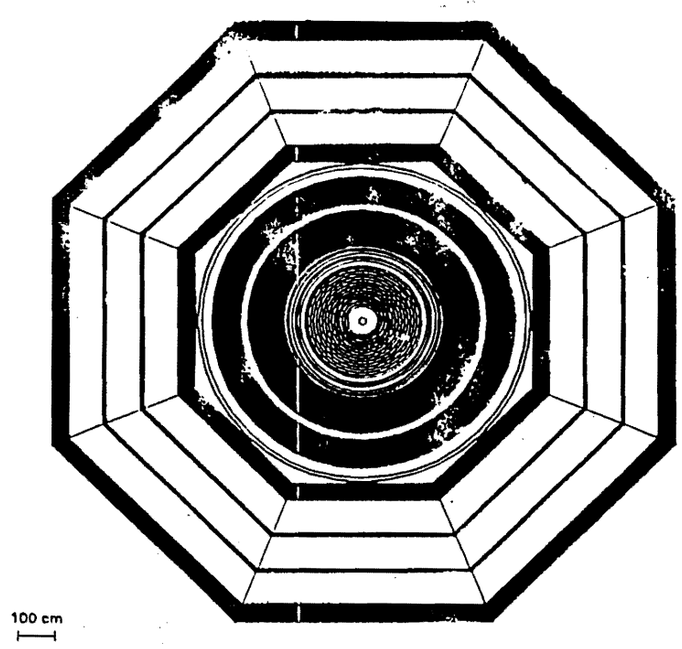

Fig.12.

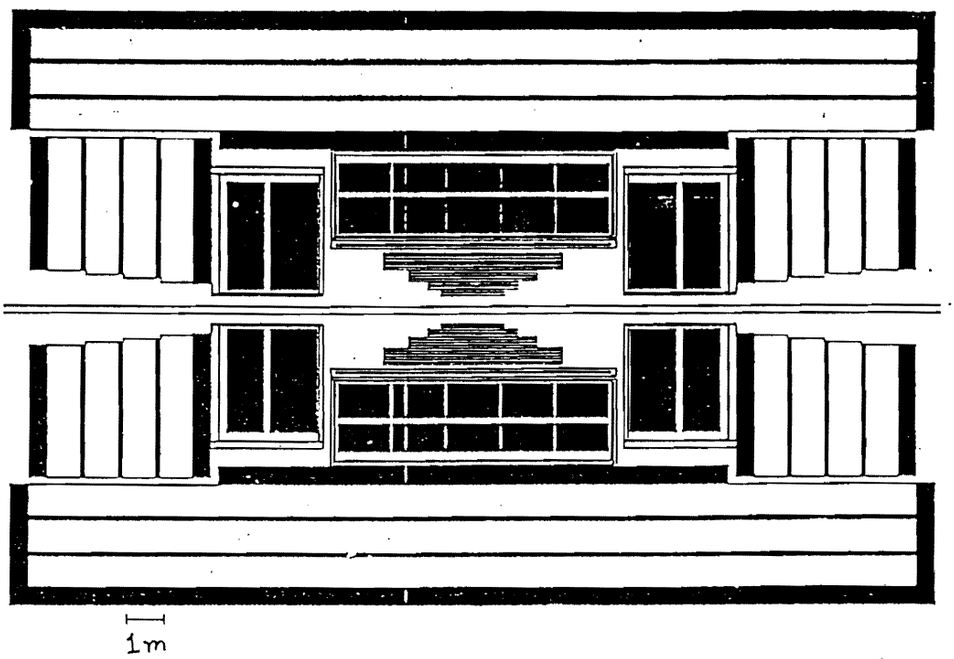

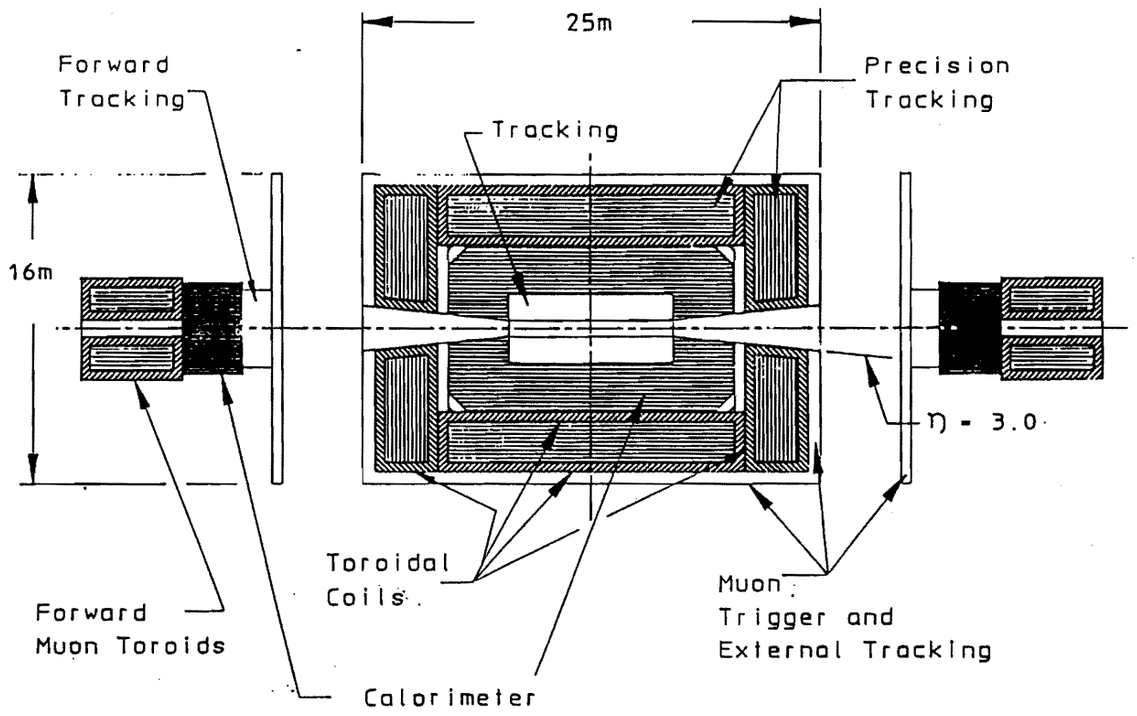
25m
Forward
Tracking
Precision
Tracking
Tracking
16m
η = 3.0
Toroidal
Coils
Forward
Muon Toroids
Muon
Trigger and
External Tracking
Calorimeter
EMPACT
MMARX prec lepin delri
MARX/CHAN 01may89

Fig.13 **Ref.12.**

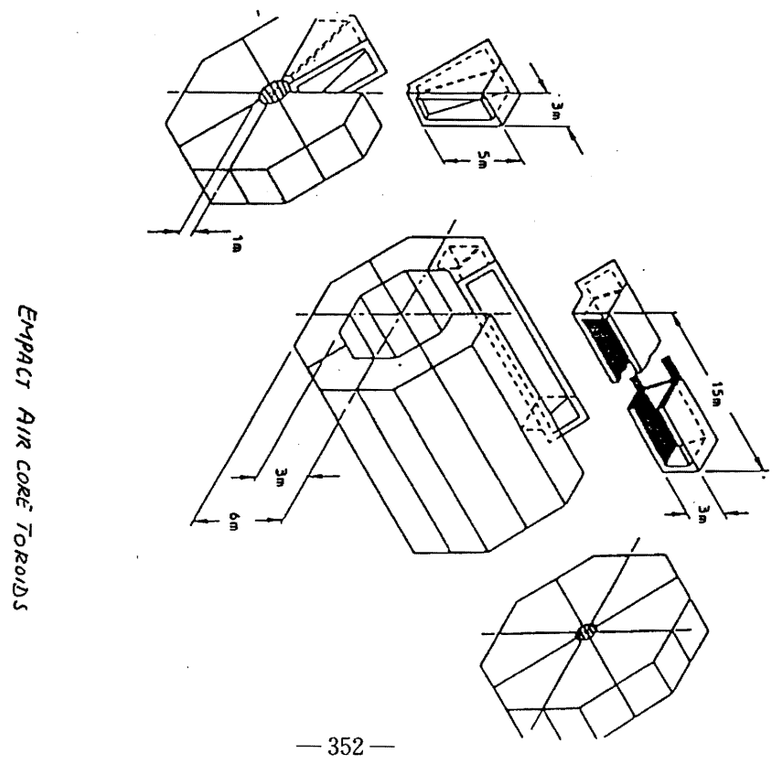
3m
5m
1m
3m
6m
15m
3m
EMPACT AIR CORE TOROIDS

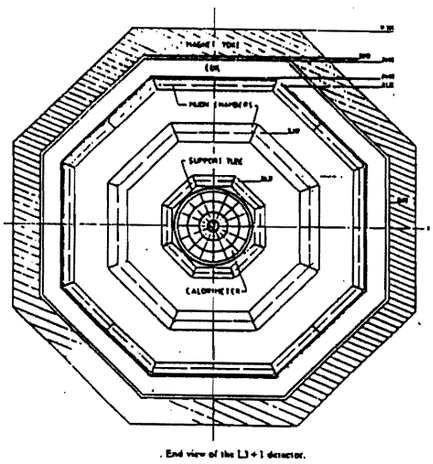

End view of the L3 + 1 detector.

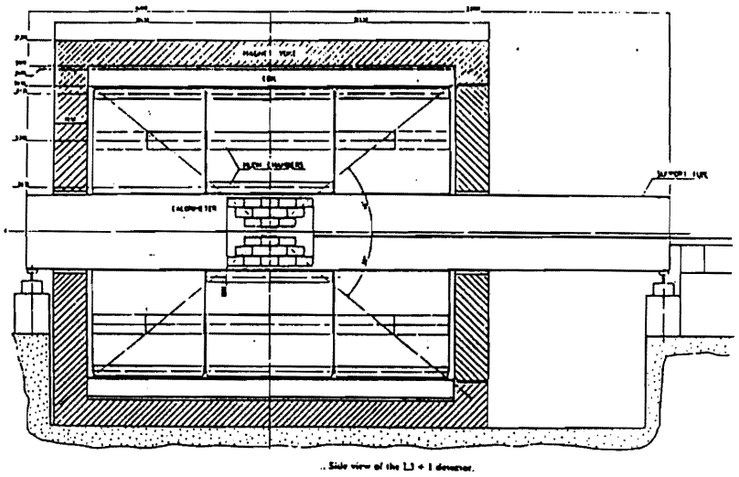

Side view of the L3 + 1 detector.

L3+1 DETECTOR

Ref.13.

Fig.14.

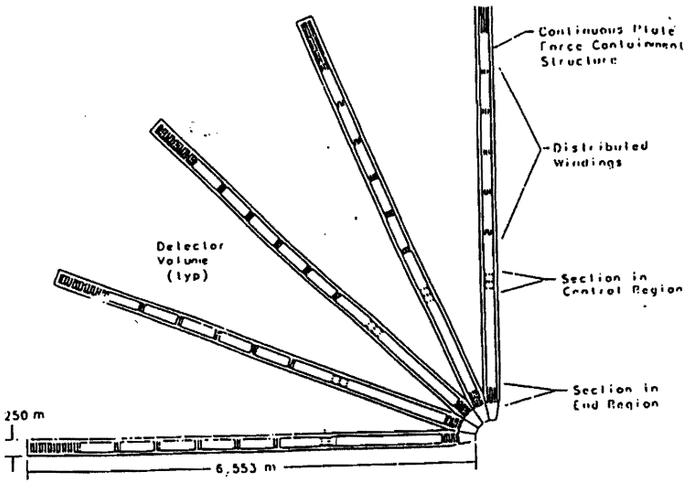

one quadrant of 16 coil array

End view of radially distributed toroidal coils, which gives uniform azimuthal field.

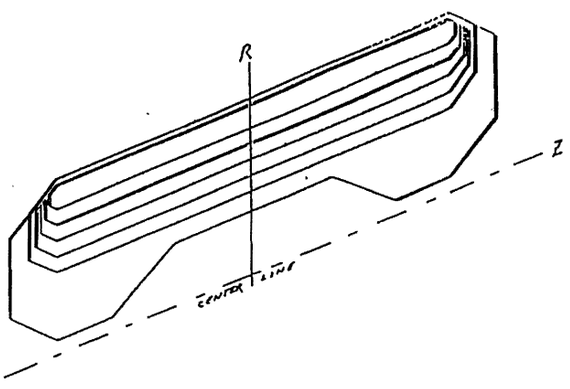

One of Sixteen Coils

Isometric view of one of the radially distributed toroidal coils, which gives uniform azimuthal field.

Ref.14.

RADIALLY DISTRIBUTED TOROIDAL COIL

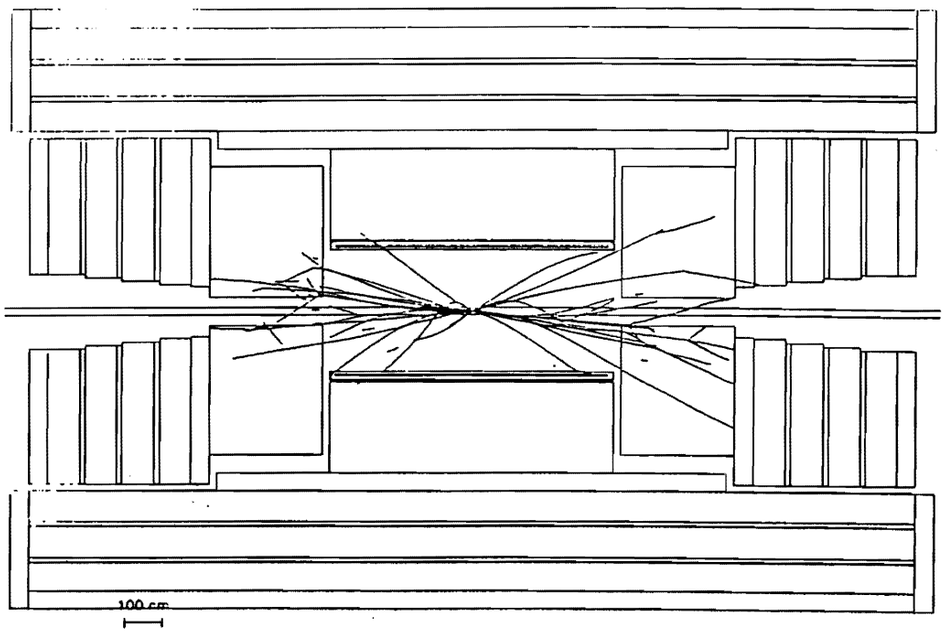

Minimum Bias Event

Fig.15.

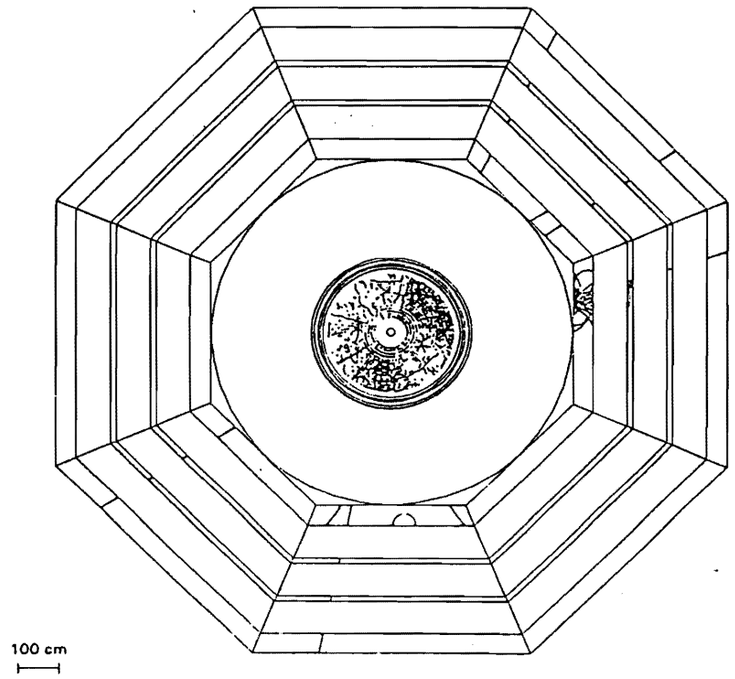

$p\bar{p} \to WW \to H^0 \to Z^0 Z^0 \to 4\mu$